Available online at www.sciencedirect.com
ScienceDirect
Precision Engineering 32 (2008) 239–250
PRECISION ENGINEERING
www.elsevier.com/locate/precision

Review

A novel 5DOF thin coplanar nanometer-scale stage

Wen-Yuh Jywe [a,*], Yeau-Ren Jeng [b], Chien-Hung Liu [c], Yun-Feng Teng [b], Chia-Hung Wu [d], Hung-Shu Wang [d], Yi-Jou Chen [a]

[a] *Department of Automation Engineering, National Formosa University, Taiwan*
[b] *Institute of Mechanical Engineering, National Chung Cheng University, Taiwan*
[c] *Institute of Electro-Optical and Materials Science, National Formosa University, Taiwan*
[d] *Department of Mechanical Engineering, National Cheng Kung University, Taiwan*

Received 25 April 2007; received in revised form 30 October 2008; accepted 29 November 2008
Available online 19 January 2008

Abstract

To minimize the size of a stage with more DOF motion, this paper concentrates on the design, manufacturing process and control of a 5DOF thin coplanar nanometer-scale stage with high accuracy and multiple DOF motion. This paper uses the features of a flexible structure to develop a 200 mm × 200 mm × 35 mm thin coplanar nanometer-scale stage with 5DOF that allows the increase or decrease of axis action in accordance with various needs. The flexible structure of the thin coplanar nanometer-scale stage includes a cylindrical flexible body and an arc flexible body. The thin coplanar nanometer-scale stage allows for three-translational and two-rotational motions and is provided with eight piezoelectric actuators—one on the *X*-axis, another on the *Y*-axis, and the others on the *Z*-axis. The displacement characteristics of the output member of the stage were measured with the built-in capacitive sensors. It also used an analysis and identification controller design method for piezoelectric actuated systems. From the results, it can be seen that the performance of this controller is good and 10 nm controlling error of the step input can be obtained. The controlling error of the rotational angle is about 0.004 arcsec.

Keywords: Stack-type stage; Flexure hinge; Nanometer stage; Piezoelectric; Positioning control

Contents

* Corresponding author. Fax: +886 5 6331211.
E-mail address: jywe@nfu.edu.tw (W.-Y. Jywe).

0141-6359/$ – see front matter © 2008 Elsevier Inc. All rights reserved.
doi:10.1016/j.precisioneng.2007.11.001

1. Introduction

In recent years, as the result of rapid developments in various fields of precision engineering, there has been a big increase in the need for precision positioning and scanning systems capable of nanometer or, sometimes, even sub-nanometer resolution and repeatability. This trend is expected to grow, requiring new design concepts and techniques for exploration of more novel devices to meet the demands of various applications. The development of precision machines is important to the study of nanometer-scale manufacturing and research. Ultra-precision stage positioning and nano-measurement technology are two key points in the domain of nanotechnology. For an ultra-precision positioning stage to achieve nanometer accuracy, piezoelectric actuators are commonly used because they have nanometer resolution [1–7]. Recently, the development of a long-range ultra-precision positioning stage has been an important target in the field of nanometer science and technology. Chang et al. [8–12] developed a micropositioning stage with a large travel range. Their stage combines a piezoelectric driving device, flexure pivoted multiple Scott–Russell linkage, and a parallel guiding spring. In 2004, Jywe et al. [13] proposed a new design method of the nanometer positioning stage, which concentrated on the design and manufacturing process of a stack-type nanometer positioning stage with high accuracy and multiple DOF for a heavy-loading machine. No previous work was found on the thinking of the volume of the stage, which might be employed on some applications such as on the application of the stage on an AFM or SPM system. Thus, a thin coplanar nanometer-scale stage could be designed.

In this paper, a flexure hinge-based stack-type 5DOF thin coplanar nanometer-scale stage with high accuracy and multiple DOF is developed. In order to simplify the structure of the stage, the cylindrical flexible body and arc flexible body are the main structures of the designed stage. Actuation of this nano-stage is done with piezoelectric actuators. Capacitive sensors are used for position measurement. The measuring system with multiple capacitance sensors for simultaneously measuring the multi-degrees-of-freedom motion errors is designed and integrated in the stage. Thus, precision positioning feedback can be obtained from the capacitance sensors. Firstly, the structure of this thin coplanar nanometer-scale stage is described. Then, the open-loop system characteristics are experimentally investigated. Based on the results of this investigation, each pair of piezoelectric actuators and corresponding capacitance sensors is treated as an independent system and modeled as a first-order linear model with hysteresis nonlinearity. The method of the analysis and identification for a hysteresis system was used to design a feedforward controller [14], and a PI controller was also designed.

2. The structure of the thin coplanar nanometer-scale stage

In this paper, the main purpose of the stage was to provide a micro-translation structure which could improve positioning accuracy and practicality. The thin coplanar nanometer-scale stage designed in this paper is a monolithic structure comprising medium carbon steel. The procedure used uses the features of a flexible structure to develop a thin coplanar nanometer-scale stage. The flexible structure of the thin coplanar nanometer-scale stage included a cylindrical flexible body and an arc flexible body. There are many parts to the flexible structure in the thin coplanar nanometer-scale stage. This flexible structure was assembled by a pre-baking process. It is composed of eight piezoelectric actuators, six adjusted mechanisms, six capacitance sensors, a rigid base, four arc flexure bodies and one four-sided flexure hinge fixture, as shown in Fig. 1. The process used the features of a flexible structure to develop a thin coplanar nanometer-scale stage with 5DOF that allows the increase or decrease of axis action in accordance with various needs. The thin coplanar nanometer-scale stage allows for three-translational and two-rotational motions and is provided with eight piezoelectric actuators—one on the *X*-axis, another on the *Y*-axis, and the others on the *Z*-axis. The displacement characteristics of the output member of the stage were measured with the built-in capacitance sensors. The measuring range of the Physik Instrumente D-015 is 15 μm. A total of six sensors were installed to measure the displacement in the *X*-axis, *Y*-axis and *Z*-axis and rotational motion along the *X*-axis (θ_x) and *Y*-axis (θ_y). The piezoelectric actuators were fastened at each end to the rigid base using the adjusted preload mechanisms. Four piezoelectric actuators (PZT1, PZT3, PZT5 and PZT7) were used to provide the translational motion of the *X*- and *Y*-axis, and another four piezoelectric actuators (PZT2, PZT4, PZT6 and PZT8) were used to provide the translational motion of the *Z*-axis and the rotational motion of the *X*- and *Y*-axis. Piezoelectric actuators are known for the unique features of compact size, swift response, high resolution, electrical mechanical coupling efficiency, and low heat. Therefore, this paper describes the use of piezoelectric actuators instead of conventional actuators.

2.1. The working principle of the thin coplanar nanometer-scale stage

The thin coplanar nanometer-scale stage has five-degrees-of-freedom performance by using different parts of piezoelectric actuators (PZT1, PZT2, PZT3, PZT4, PZT5, PZT6, PZT7 and PZT8) to push the flexible body. There are two piezoelectric actuators (PZT1 and PZT5) on the *X*-axis. By using the piezoelectric actuators (PZT1 and PZT5), the stage could be made to move when the PZT1 pushed the four-sided flexure hinge fixture or the other PZT5 pushed the four-sided flexure hinge fixture. There are also two piezoelectric actuators (PZT3 and PZT7) on the *Y*-axis. By using the piezoelectric actuators (PZT3 and PZT7), the stage could be made to move when the PZT3 pushed the four-sided flexure hinge fixture or the other PZT7 pushed the four-sided flexure hinge fixture. There are four piezoelectric actuators (PZT2, PZT4, PZT6 and PZT8) on the *Z*-axis. When the four piezoelectric actuators (PZT2, PZT4, PZT6 and PZT8) pushed the arc flexure bodies, these bodies become and the platform rose. The schematic drawing is shown in Fig. 2. When the two piezoelectric actuators (PZT6 and PZT8) pushed the arc flexure bodies, the platform rose and the rotational angle θ_x

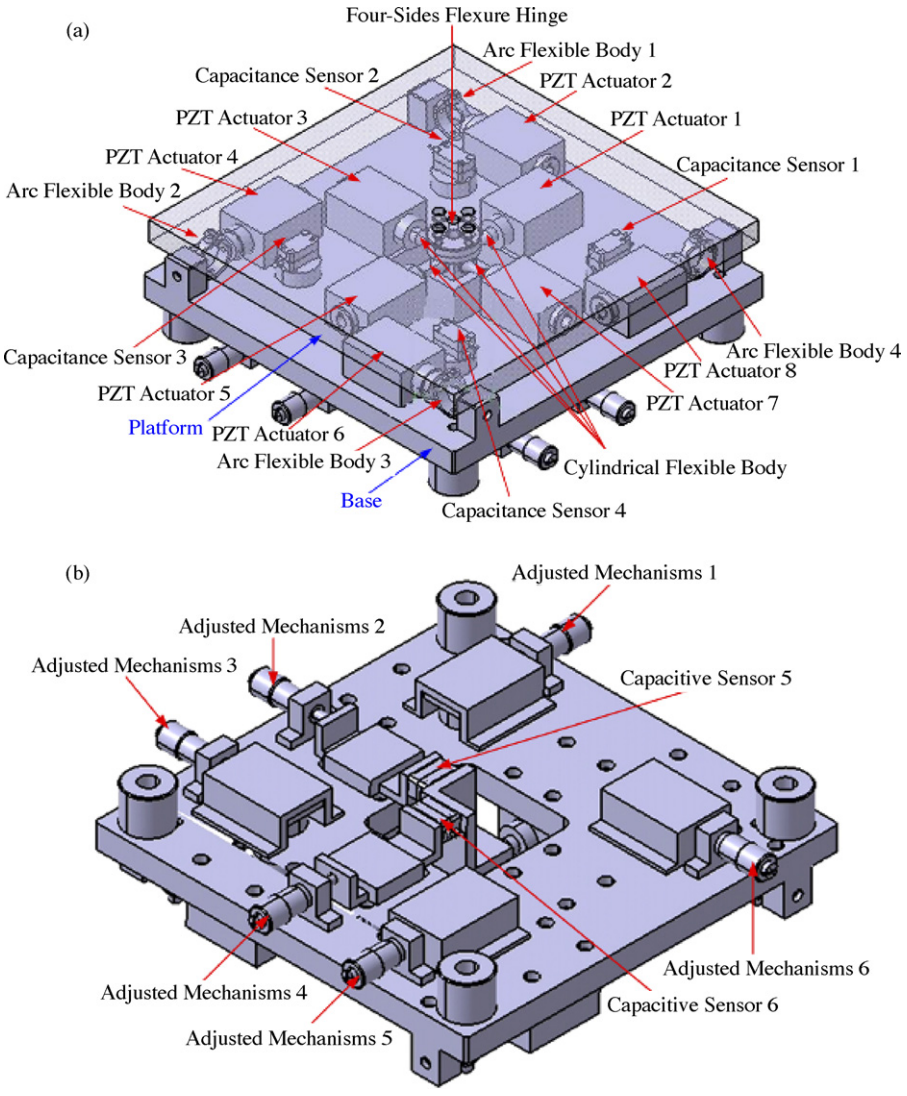

Fig. 1. Schematic drawing of the thin coplanar nanometer-scale stage. (a) The inside structure of the stage and (b) the back structure of the stage.

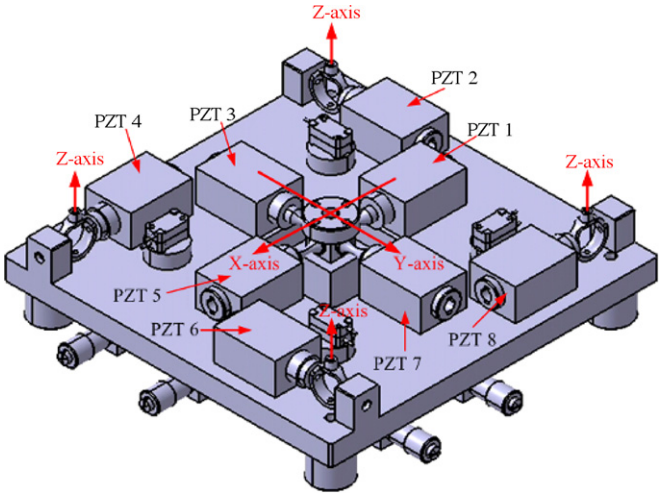

Fig. 2. Schematic drawing of the thin coplanar nanometer-scale stage motion axis.

was reduced. When the two piezoelectric actuators (PZT2 and PZT8) pushed the arc flexure bodies, the platform also rose and the rotational angle θ_y was reduced. The schematic drawing is shown in Fig. 3.

2.2. *Flexible body*

There are many parts to the flexible structure of the thin coplanar nanometer-scale stage. The thin coplanar nanometer-scale stage is provided with a flexible body as its major framework. Because the dimension of the flexible body will affect the displacement result of the stage, it is necessary to determine the dimension of the flexible structure and to find out the exact amount of displacement. This paper analyzes the dimension of the flexible structure so as to find out the proper dimension of displacement. In this paper, there are two kinds of flexible body in the thin coplanar nanometer-scale stage. The structure is shown in Fig. 4. CATIA was used to simulate the dimension of the flexible body so as to find out the proper dimension of displacement.

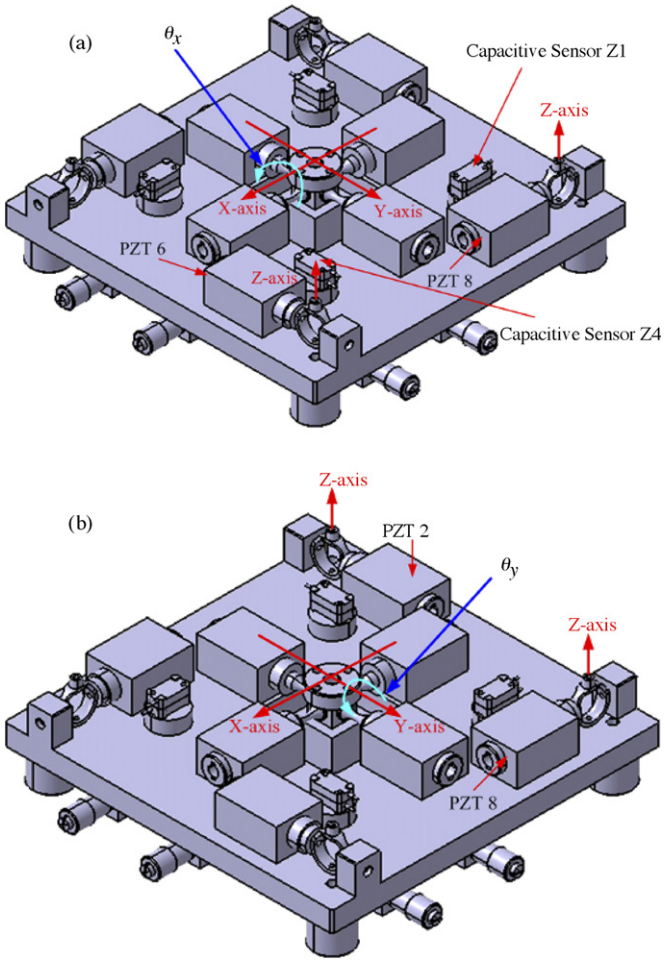

Fig. 3. Schematic drawing of the thin coplanar nanometer-scale stage motion axis. (a) The rotational angle θ_x and (b) the rotational angle θ_y.

2.3. Actuator

Piezoelectric actuators provide high stiffness and resolution but can also have an amount of hysteresis with a relatively short displacement range. The Piezomechanik GmbH PSt150/7/20 Vs12 is 28-mm long with an outside diameter of 12 mm. The electrodes of the actuator were deposited in the outside and inside surfaces of the PZT tube, which provided a maximum displacement of 20 μm with an excitation of 150 V.

2.4. Capacitance sensor

The displacement characteristics of the output member of the stage were measured with the built-in capacitance sensors. The Physik Instrumente D-015 has a displacement resolution of 0.01 nm. The total range of the capacitance sensors was 15 μm with a sensitivity of 0.66 V/μm. A total of six capacitance sensors were installed to measure the displacement in the *X*-axis, *Y*-axis and *Z*-axis and rotation in the θ_x axis and θ_y axis. The sensors for the *X*-axis and *Y*-axis were placed as close as possible to the symmetry axis of the stage to reduce Abbe errors.

3. The assembly process of the thin coplanar nanometer-scale stage

The coplanar nanometer-scale stage described in this study comprises a number of components. The cylindrical flexible body and four piezoelectric actuators were assembled first. The four piezoelectric actuators were assembled with the holders. There are adjustment mechanisms in the back of the holder to provide the piezoelectric actuators with the preload. In the assembly process of the arc flexible body, the arc flexible body was assembled with the PZT holder and the piezoelectric actuator. The arc flexible body was also assembled with the holder and the adjustment mechanism. In the final assembly process, the structure of the cylindrical flexible body and the arc flexible body were assembly on a rigid base. At the same time, the capacitance sensors were also assembled in the structure of the thin coplanar nanometer-scale stage. In the final step, the platform was tied together with the cylindrical flexible body. Fig. 5 shows the assembly process of the thin coplanar nanometer-scale stage and Fig. 6 shows a photograph of the thin coplanar nanometer-scale stage.

4. The measuring system

In this paper, a measuring system is developed using six capacitance sensors. Four capacitance sensors were installed

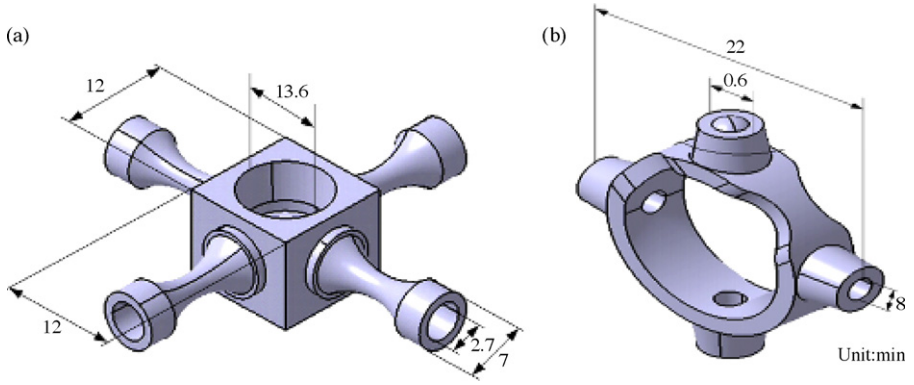

Fig. 4. Schematic drawing of the flexible body: (a) cylindrical flexible body and (b) arc flexible body.

inside the structure of the thin coplanar nanometer-scale stage and two capacitance sensors were installed at the back of the structure. The schematic drawing is shown in Fig. 9. The displacement characteristics of the output member of the stage were measured with the built-in capacitance sensors. Two capacitance sensors were installed at the back of the structure of the thin coplanar nanometer-scale stage to measure the displacement of the *X*-axis and *Y*-axis. Four capacitance sensors were installed

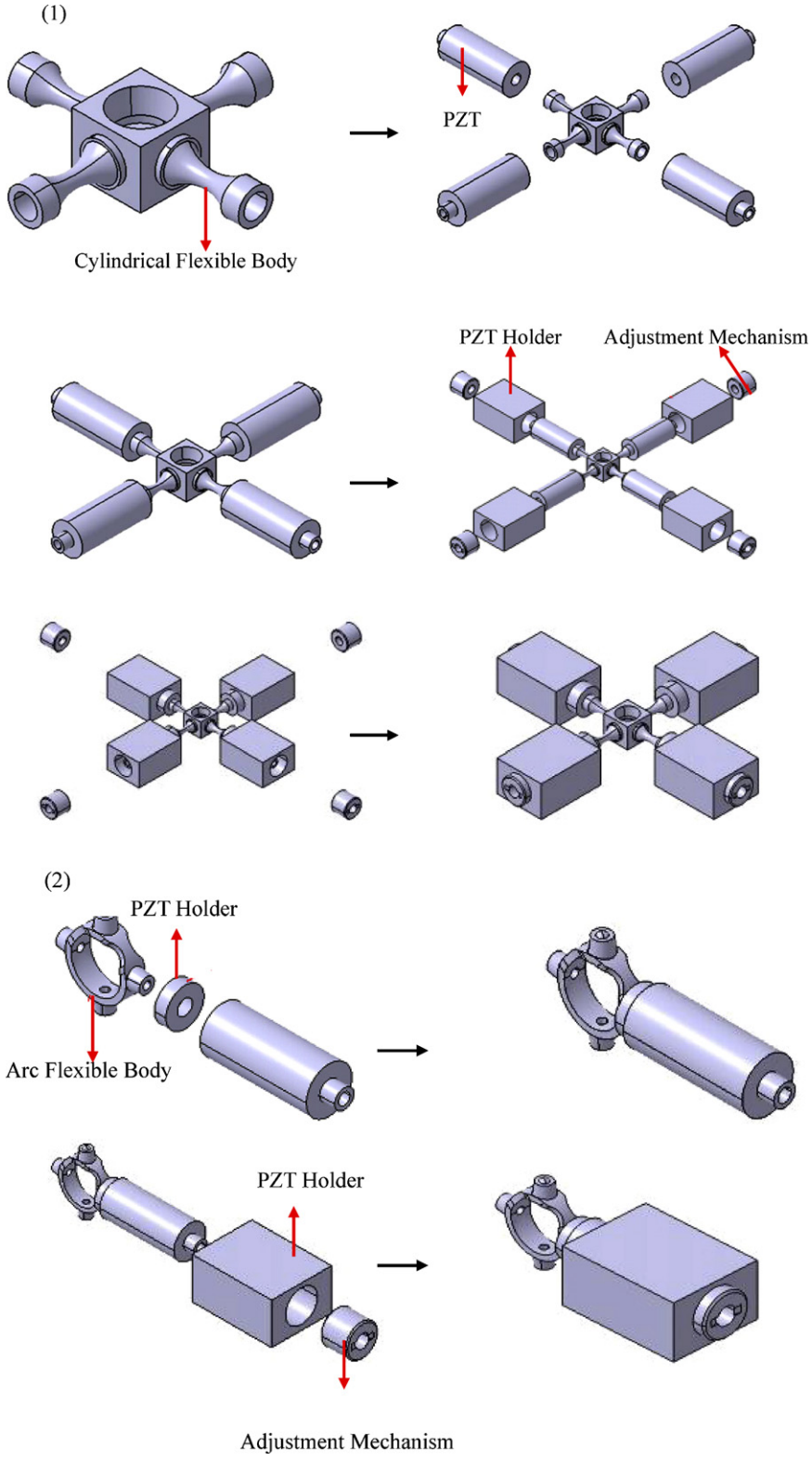

Fig. 5. The assembly process of the thin coplanar nanometer-scale stage. (1) The assembly process of the cylindrical flexible body. (2) The assembly process of the arc flexible body. (3) The assembly process of the thin coplanar nanometer-scale stage.

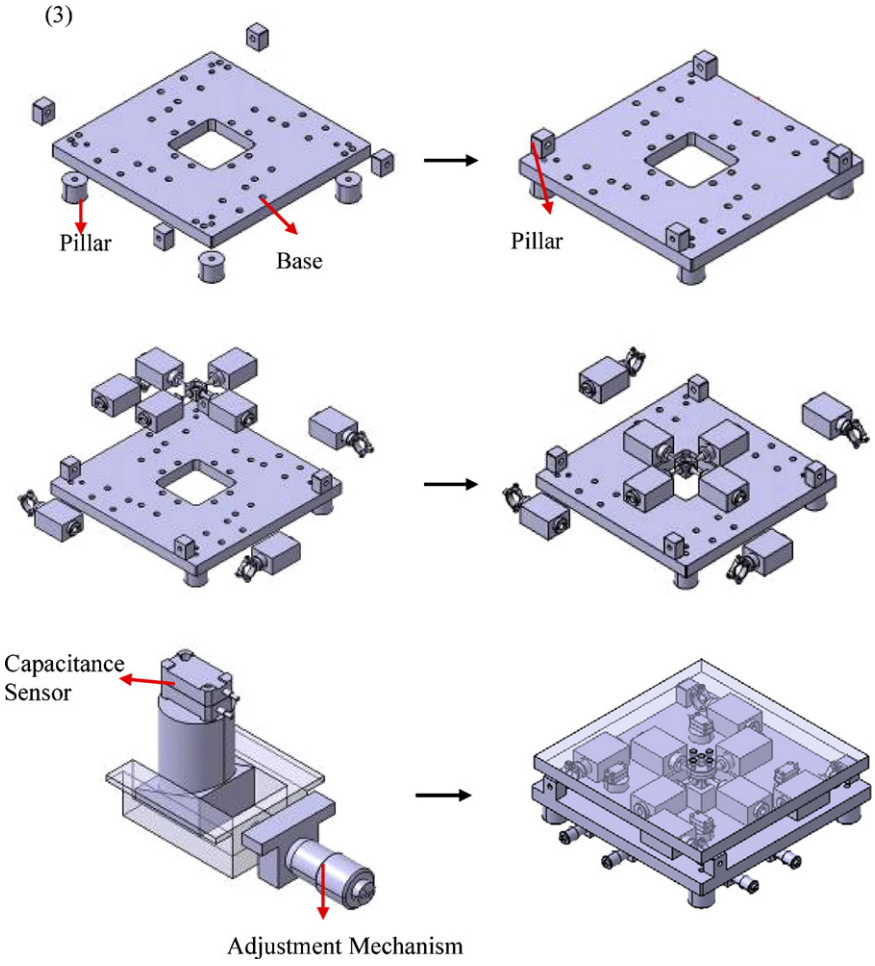

Fig. 5. (*Continued*)

inside the structure of the thin coplanar nanometer-scale stage to measure the displacement of the Z-axis and rotational motion along the X-axis (θ_x) and Y-axis (θ_y) (Fig. 7).

The relation of the rotational angle θ_x and θ_y between the displacement measured by the capacitance sensor $Z1$, $Z2$, $Z3$, $Z4$ and the displacement of the center of the stage platform in the Z-axis can be obtained as $Z1 = Z + r_1 \sin\theta_x + r_2 \sin\theta_y$, $Z2 = Z + r_1 \sin\theta_x - r_2 \sin\theta_y$, $Z3 = Z - r_1 \sin\theta_x - r_2 \sin\theta_y$ and $Z4 = Z - r_1 \sin\theta_x + r_2 \sin\theta_y$, respectively. The distance of r_1 or r_2 (38.5 mm) is half the distance between the center of sensors $Z1$ and $Z2$ or $Z3$ and $Z4$. Note that θ_x is small, therefore, $\sin\theta_x \approx \theta_x$.

The geometric relation is shown in Fig. 8. The relations between $Z1$, $Z2$, $Z3$, $Z4$, Z, θ_x and θ_y can be summarized as

$$\begin{bmatrix} X \\ Y \\ Z1 \\ Z2 \\ Z3 \\ Z4 \end{bmatrix} = \begin{bmatrix} 1 & 0 & 0 & 0 & 0 \\ 0 & 1 & 0 & 0 & 0 \\ 0 & 0 & 1 & r_1 & r_2 \\ 0 & 0 & 1 & r_1 & -r_2 \\ 0 & 0 & 1 & -r_1 & -r_2 \\ 0 & 0 & 1 & -r_1 & r_2 \end{bmatrix} \begin{bmatrix} X \\ Y \\ Z \\ \theta_x \\ \theta_y \end{bmatrix} \quad (1)$$

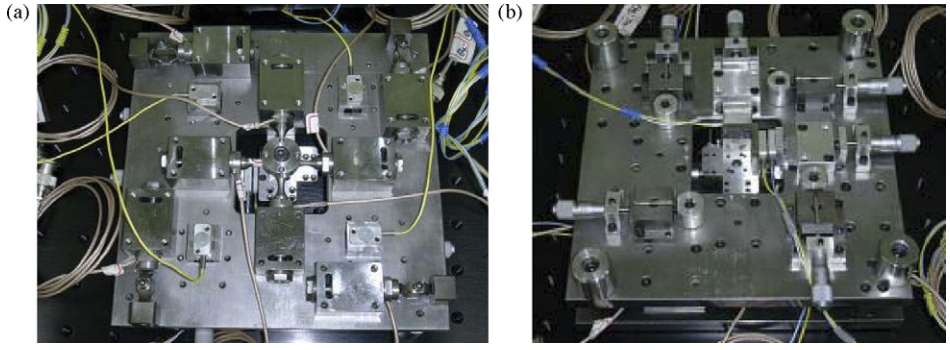

Fig. 6. Photograph of the thin coplanar nanometer-scale stage: (a) the inside structure of the stage and (b) the back structure of the stage.

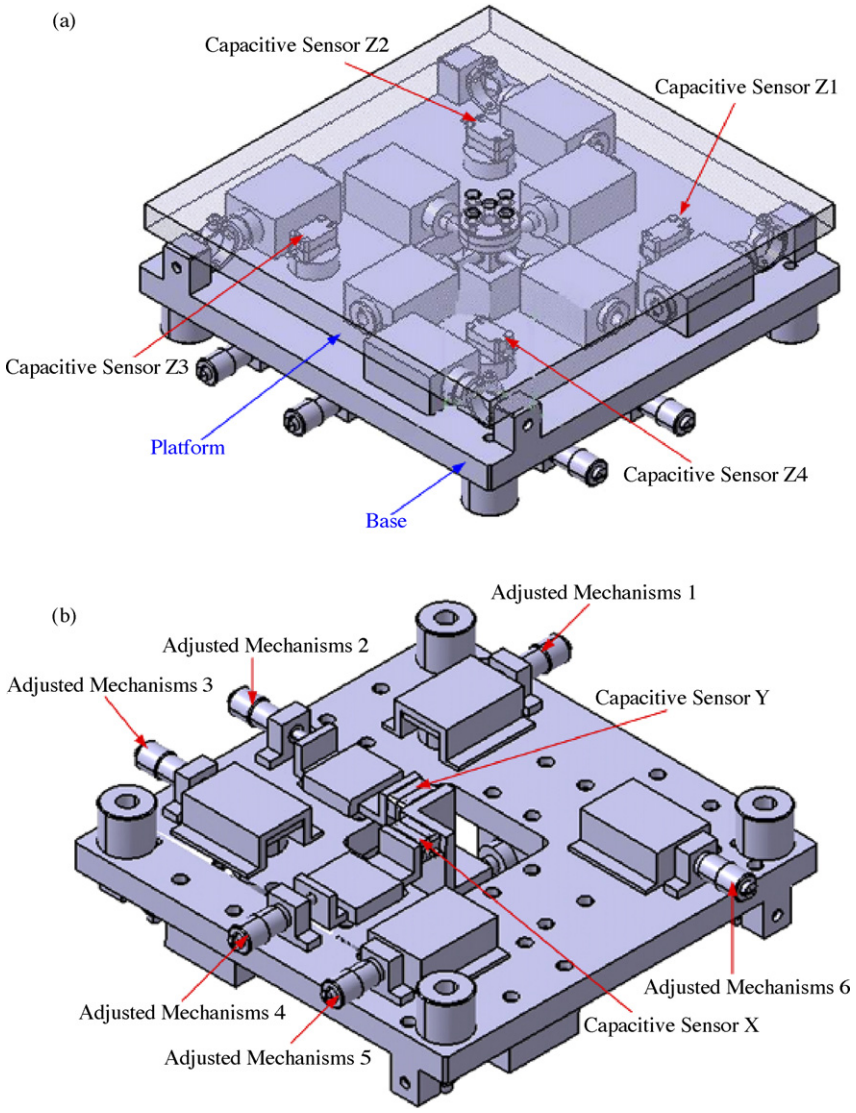

Fig. 7. Schematic drawing of the thin coplanar nanometer-scale stage: (a) the inside structure of the stage and (b) the back structure of the stage.

5. The control system

The control system is shown in Fig. 9. It includes a personal computer, a Dspace card (DS1103), an analog amplifier (SVR 150/3), eight piezoelectric actuators (PSt150/7/20 Vs12), a 5DOF thin coplanar nanometer-scale stage, six capacitance sensors (PI, D-015) and a sensor signal processor (PI, E-509). The control procedure used the MATLAB software for compiling the control blocks and compiled the DSP card (DS1103). By using the DSP card (DS1103), the control blocks could be executed and the digital/analog signals could be processed. The amplifier (SVR 150/3) supplied the required voltage to the piezoelectric actuators (PSt150/7/20 Vs12) of the 5DOF thin coplanar nanometer-scale stage. The axial displacement of the 5DOF thin coplanar nanometer-scale stage could be measured using the capacitance sensors (PI, D-015) and the signal was sent to the signal processor (PI, E-509).

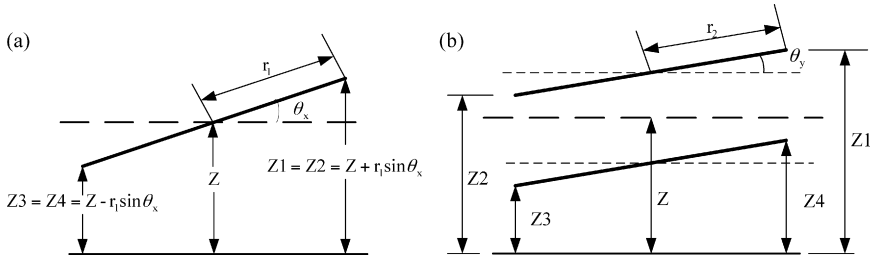

Fig. 8. The geometric relation of the $Z1$, $Z2$, $Z3$, $Z4$, θ_x and θ_y. (a) The relations between $Z1$, $Z2$, $Z3$, $Z4$ and θ_x. (b) The relations between $Z1$, $Z2$, $Z3$, $Z4$, θ_x and θ_y.

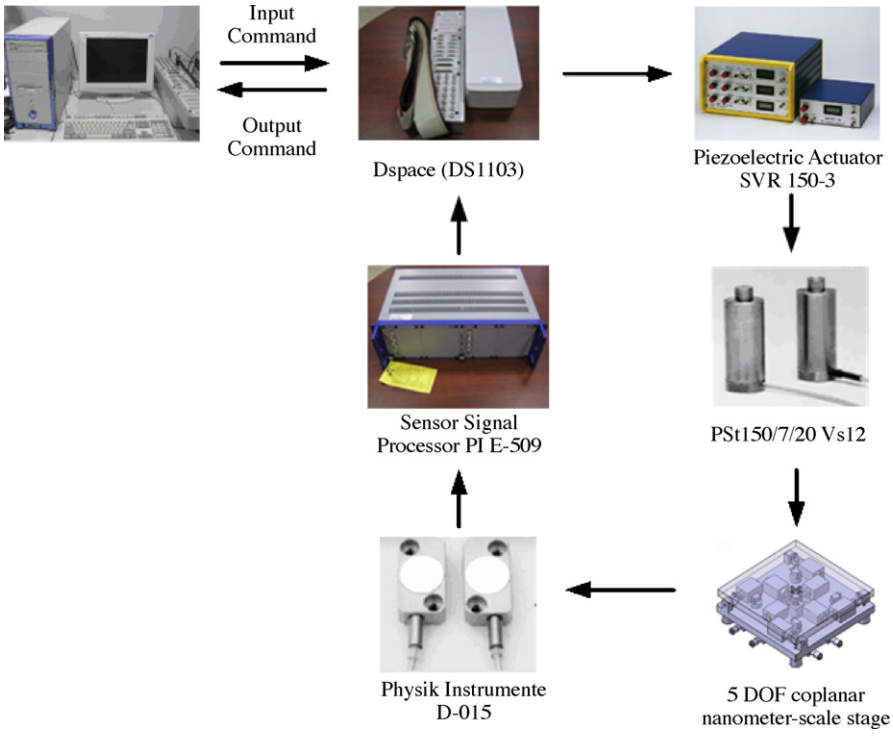

Fig. 9. Flow diagram of the system.

5.1. The open-loop dynamic characteristics of the thin coplanar nanometer-scale stage

In order to design the controller, it is necessary to understand the open-loop characteristics of the 5DOF coplanar nanometer-scale stage. Firstly, the maximum moving range and hysteresis nonlinearity of piezoelectric actuators are investigated by static tests. The testing voltage was sent to the piezoelectric actuators and the displacements measured by sensors were recorded. The test results are shown in Figs. 10–15. From the results, it is found that the moving ranges of the *X*-axis, *Y*-axis, and *Z*-axis are about 9.11, 9.71 and 5.33 μm, respectively.

6. Controlling system design

6.1. Analysis and identification for a hysteresis system

The hysteresis loop of an actuator can be obtained by measuring its displacement when its input voltage is increased and decreased. The characteristic feature of the hysteresis loop is shown in Fig. 13.

The generic model for hysteresis effects ($w(t_0) = w_0 \in R$, $v(t) \in R$):

$$\sum_{\mathrm{H}} \equiv \left\{ \frac{\mathrm{d}w(t)}{\mathrm{d}t} = h(v(t), \dot{v}(t), w(t)) \right. \tag{2}$$

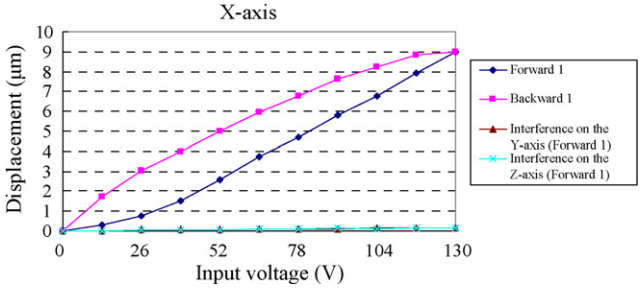

Fig. 10. The displacement of the *X*-axis and the interference of the *Y*-axis and *Z*-axis.

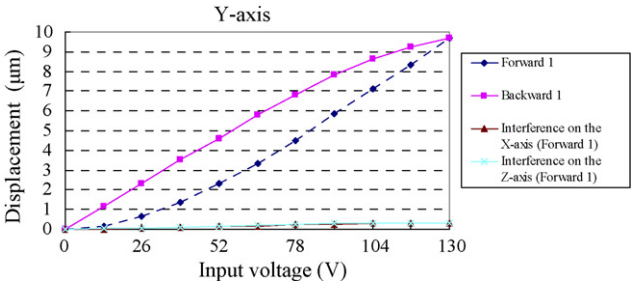

Fig. 11. The displacement of the *Y*-axis and the interference of the *X*-axis and *Z*-axis.

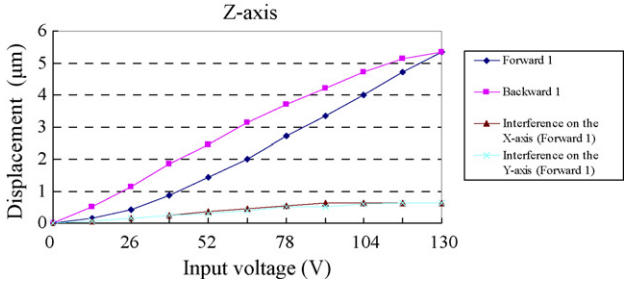

Fig. 12. The displacement of the *Z*-axis and the interference of the *X*-axis and *Y*-axis.

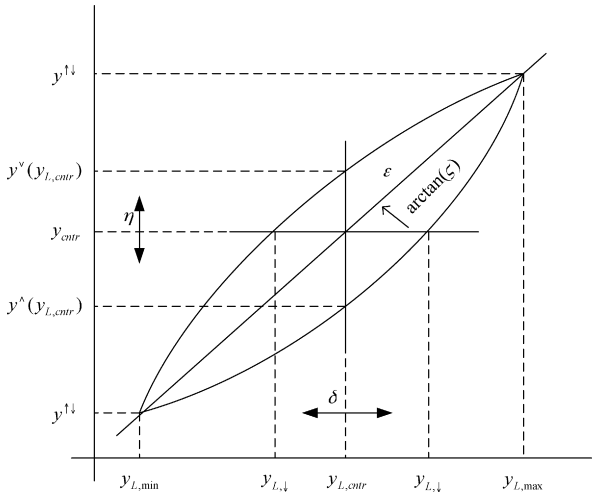

Fig. 13. Characteristic features of the hysteresis loop.

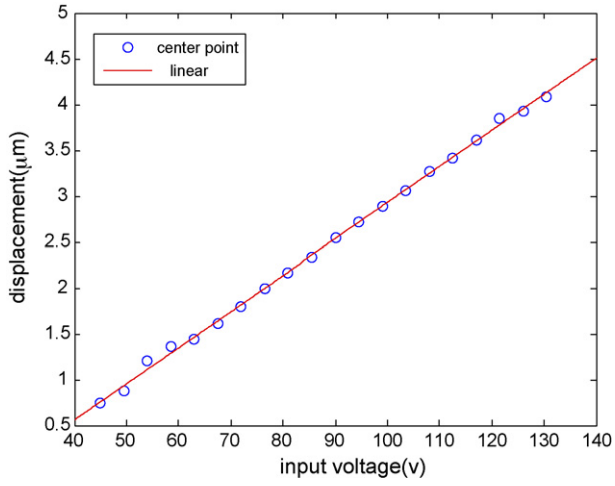

Fig. 14. Measured center point of a hysteresis loop vs. the applied voltage offset, together with the best linear approximation.

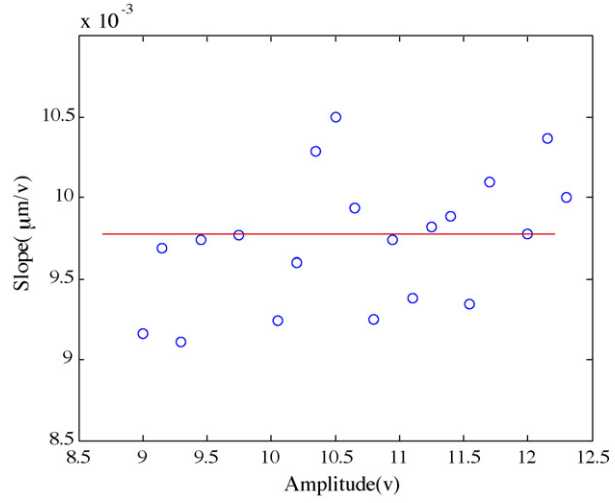

Fig. 15. Measured slope of a hysteresis loop vs. the applied voltage amplitude, and the constant average value.

with

$$h(v(t), \dot{v}, w(t)) = f(v(t), w(t))|\dot{v}(t)| + g(v(t), w(t))\dot{v}(t) \tag{3}$$

In the context of this paper, the state-space analysis and identification for the purpose of control, we only admit differential models of hysteresis based on a function $f(v(t), w(t))$ that is affine in $w(t)$, and a function $g(v(t), w(t))$ that is constant in $w(t)$. The resulting system function of the hysteresis model Σ_H is then equal to

$$h(v(t), \dot{v}, w(t)) = -\alpha w(t)|\dot{v}(t)| + \alpha|\dot{v}(t)|f(v(t)) + \dot{v}(t)g(v(t)) \tag{4}$$

With $0 < \alpha \in R$. Model Σ_H with this system function has been used to characterize physical hysteresis phenomena, provided functions $f(\cdot)$ and $g(\cdot)$ comply with [15,16]. The characteristic features can be associated with the stationary hysteresis loop of system Σ_H: a left turning point $(y_{L,\min}, y^{\downarrow\uparrow})$, a right turning point $(y_{L,\max}, y^{\uparrow\downarrow})$, a horizontal aperture δ, a vertical aperture η, a slope ζ, a hysteresis area ε and the coordinates of the center point $(Y_{L,cntr}, Y_{cntr})$ may be determined as

$$y_{L,cntr} = \tfrac{1}{2}[y_{L,\min} + y_{L,\max}], \qquad y_{cntr} = \tfrac{1}{2}[y^{\uparrow\downarrow} + y^{\downarrow\uparrow}] \tag{5}$$

and furthermore, that

$$\text{slope}: \quad \zeta \equiv \frac{y^{\uparrow\downarrow} - y^{\downarrow\uparrow}}{y_{L,\max} - y_{L,\min}} \tag{6}$$

$$\text{horizontal aperture}: \quad \delta \equiv y_{L,\uparrow} - y_{L,\downarrow} \tag{7}$$

$$\text{vertical aperture}: \quad \eta \equiv y^{\downarrow}(y_{L,cntr}) - y^{\uparrow}(y_{L,cntr}) \tag{8}$$

$$\text{hysteresis area}: \quad \varepsilon \equiv \int_{-y_{L,\max}}^{-y_{L,\min}} y^{\downarrow}([-y_L])\,\mathrm{d}[-y_L] - \int_{y_{L,\min}}^{y_{L,\max}} y^{\uparrow}(y_L)\,\mathrm{d}y_L \tag{9}$$

In the testing experiment, a low frequency triangle wave was used to drive the piezoelectric actuators, respectively, and the

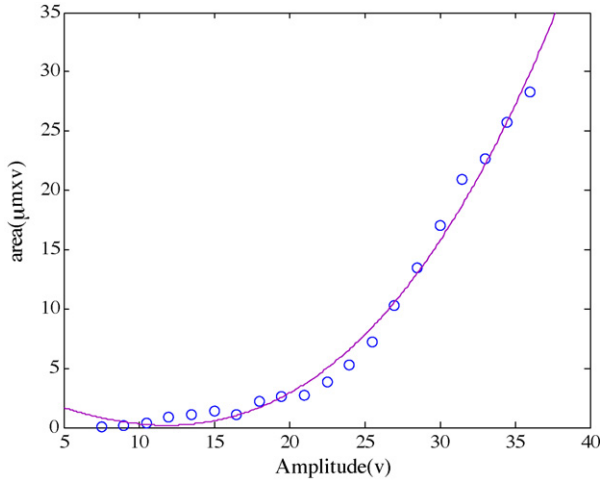

Fig. 16. Measured hysteresis area of a hysteresis loop vs. the applied voltage amplitude, and the optimal theoretical fit.

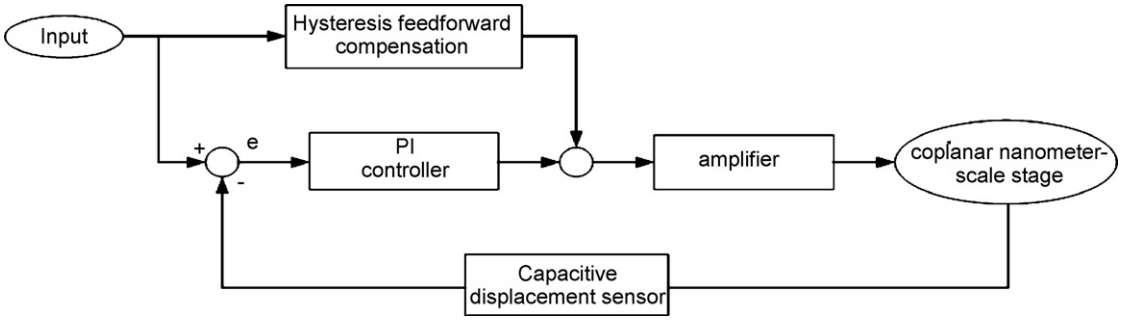

Fig. 17. Block diagram of closed loop control of the thin coplanar nanometer-scale stage.

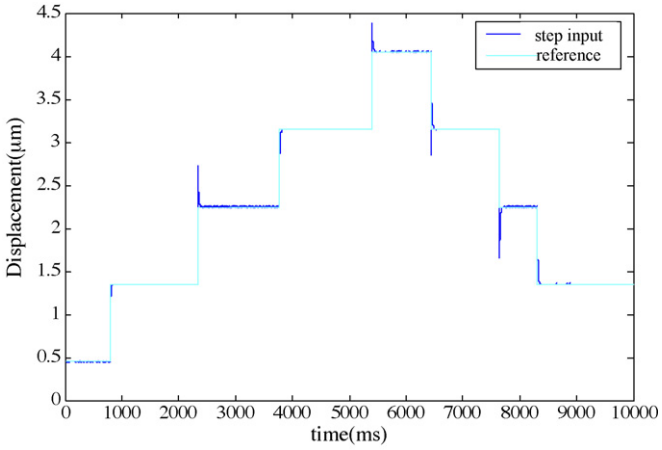

Fig. 18. The control result of the step input.

displacements measured by the sensors were recorded. Let the sinusoidal input signal $u(t) = \bar{u} + A\sin(\omega t)$ for the overall system dynamics be such that $Y_L(t) = u(t)$. The center point of the hysteresis loop in the u/y plane is then $(\bar{u}, a\bar{u})$. The remaining characteristic features of the hysteresis loop can be determined as

$$\zeta = a + \frac{b-a}{\alpha}\frac{1-\mathrm{e}^{-2\alpha A}}{A(1+\mathrm{e}^{-2\alpha A})} \approx b \tag{10}$$

$$\delta \approx 2\frac{a-b}{\alpha}\frac{(1-\mathrm{e}^{-\alpha A})^2}{a(1-\mathrm{e}^{-\alpha A})^2 + 2b\,\mathrm{e}^{-\alpha A}} \approx \alpha\left(\frac{a}{b}-1\right)A^2 \tag{11}$$

$$\eta = 2\frac{a-b}{\alpha}\frac{(1-\mathrm{e}^{-\alpha A})^2}{1+\mathrm{e}^{-2\alpha A}} \approx \alpha(a-b)A^2 \tag{12}$$

$$\varepsilon = 4\frac{a-b}{\alpha}\left\{A - \frac{1}{\alpha}\frac{1-\mathrm{e}^{-2\alpha A}}{1+\mathrm{e}^{-2\alpha A}}\right\} \approx \frac{4}{3}(a-b)\alpha A^3 \tag{13}$$

The approximations are valid for $\alpha A \ll 1$.

The differential model of hysteresis Σ_H is rewritten as

$$\sum_H = \frac{\mathrm{d}w(t)}{\mathrm{d}t} = -\alpha w(t)|\dot{v}(t)| + \alpha a v(t)|\dot{v}(t)| + b\dot{v}(t) \tag{14}$$

Application of a voltage signal $u(t) = \bar{u} + A\sin(\omega t)$, $\omega = 0.2\pi$ (rad/s) to the piezoelectric actuators driving the thin coplanar nanometer-scale stage yielded a stationary system

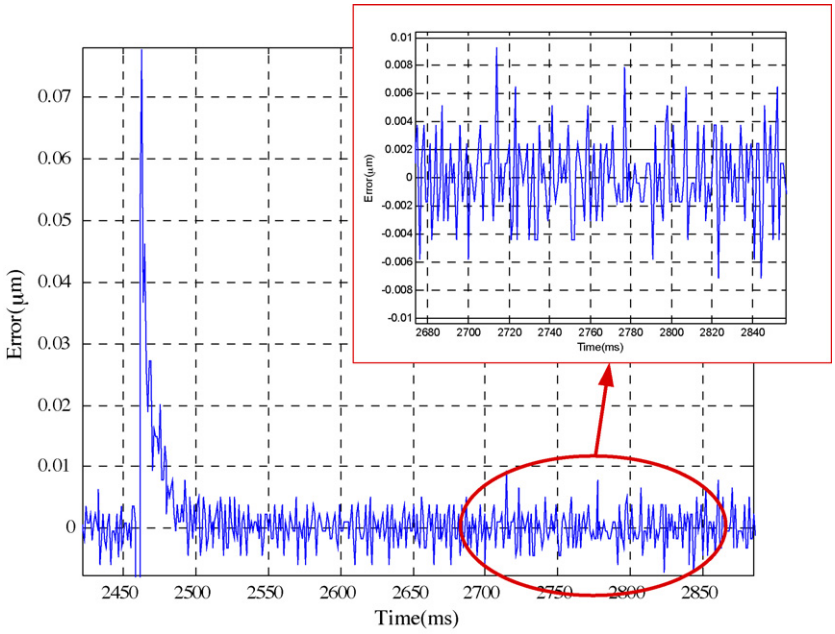

Fig. 19. The positioning error of the step input.

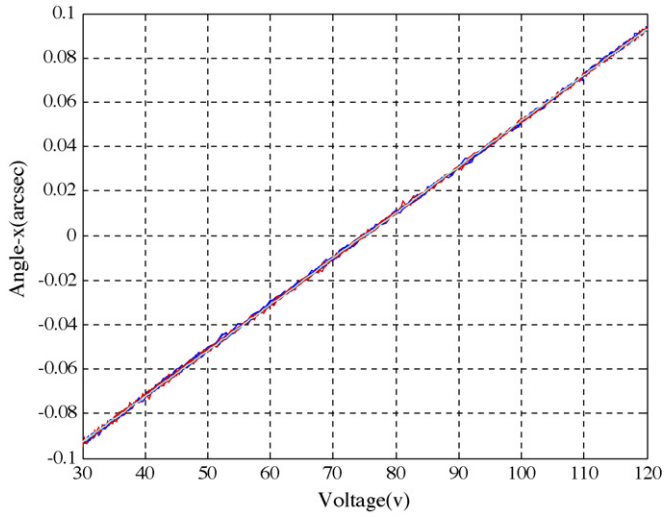

Fig. 20. The performance of the rotational angle θ_x using the closed loop control.

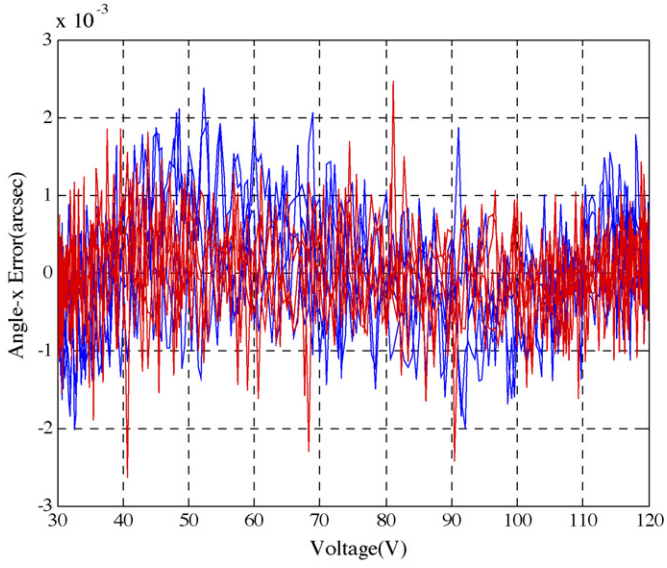

Fig. 21. The controlling error of the rotational angle θ_x.

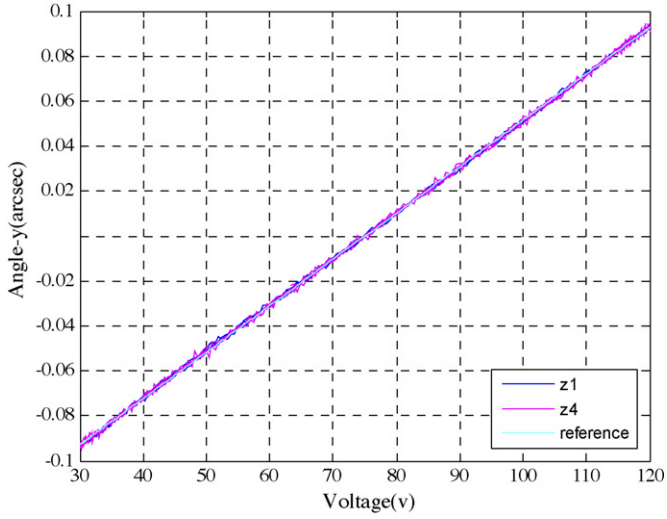

Fig. 22. The performance of the rotational angle θ_y using the closed loop control.

Table 1
Parameters of the differential model of hysteresis

a	0.029
b	0.082
α	0.063

response $y(t)$. In order to determine the parameter a, an experiment was conducted in which only offset $\bar{u}$ was varied. The results of this experiment are shown in Fig. 14. The open circlets represent empirically obtained center points while the solid line represents a first order least-squares approximation. When the amplitude A of the input signal is small enough, the slope of the hysteresis loop is equal to b. The experimental slope values are shown in Fig. 15. The parameter α can be determined from the fit of expression (13) to a series of experimentally determined values for ε. The measured hysteresis area of the hysteresis loop is shown in Fig. 16. The values of parameters a, b and α determined in these fashions are available in Table 1.

6.2. Controller design

Hysteresis was measured by applying a 0.1 Hz sinusoidal signal to the piezoelectric actuator and the displacements were measured by the built-in capacitance sensor. The method of analysis and identification for a hysteresis system was used to design a feedforward controller and a PI controller. The block diagram is shown in Fig. 17.

6.3. Experimental results

The experimental results are shown in Figs. 18–23. Figs. 18 and 19 are the trajectory results of the step input. It can be seen that the axis can track the desired trajectory very well. The positioning error of the step input is about 13 nm. Figs. 20 and 22 show the performance of the rotational angle θ_x

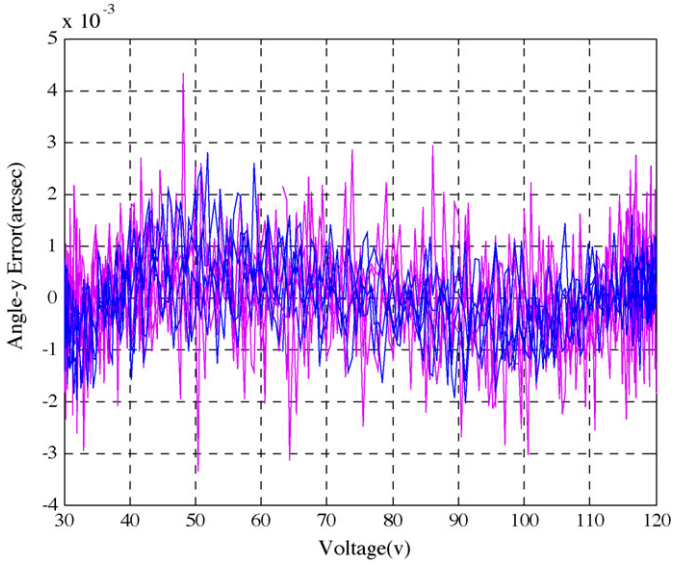

Fig. 23. The controlling error of the rotational angle θ_y.

and θ_y by using the closed loop control. It can be concluded that the controlling error is about 4 arcsec.

7. Conclusion

This paper describes the successful design and development of a 200 mm × 200 mm × 35 mm 5DOF thin coplanar nanometer-scale stage using the cylindrical flexible body and arc flexible body. The coplanar nanometer-scale stage was experimentally tested using the built-in capacitance sensor. As indicated by the experimental results, the stage's displacement reached 9.11 μm along the *X*-axis, 9.71 μm along the *Y*-axis, and 5.33 μm along the *Z*-axis. This article also illustrates an analysis and identification controller design method for piezoelectric actuated systems, which was then used to design the controllers for a thin coplanar nanometer-scale stage. From the result it can be seen that the performance of this controller is good and 10 nm controlling error of the step input can be obtained. The controlling error of the rotational angle is about 0.004 arcsec.

Acknowledgment

The work was supported by the National Science Council, Taiwan, Republic of China (number NSC 95-2221-E-150-052).

References

[1] Goto H, Sasaoka T. Vertical micro positioning system using PZT actuator. Bull Jpn Soc Prec Eng 1988;22:277–83.
[2] Taniguchi M, Ikeda M, Inagaki A, Funatsu R. Ultra precision wafer positioning by six axes micro-motion mechanism. Int J Jpn Soc Prec Eng 1992;26:35–40.
[3] Henmi N, Sato K, Wada S, Shimikohbe A. A six degrees of freedom fine motion mechanism. Mechatronics 1992;2:445–57.
[4] Schweizertr R, Yang R, Jouaneh M. Design and characterization of a low-profile micropositioning stage. Prec Eng 1996;8(1):20–9.
[5] Merkle RC. A new family of six degrees of freedom positional devices. Nanotechnology 1997;8:47–52.
[6] Chang SH, Du BC. A precision piezodriven micropositioner mechanism with large travel range. Rev Sci Instrum 1998;69(4):1785–91.
[7] Juhas L, Vuhanic A, Asamovic N, Nagy L, Borovac B. A platform for micropositioning based on piezo legs. Mechatronics 2001;11:869–97.
[8] Chang SH, Tseng CK, Chien HC. An ultra-precision *XY* θ_z piezo-micropositioner. Part I. Design and analysis. IEEE Trans Ultrason Ferroelectr Freq Control 1999;46:897–905.
[9] Chang SH, Tseng CK, Chien HC. An ultra-precision *XY* θ_z piezo-micropositioner. Part II. Experiment and performance. IEEE Trans Ultrason Ferroelectr Freq Control 1999;46:906–12.
[10] Shutov MV, Howard DL, Sandoz EE, Sirota JM, Smith RL, Collins SD. Electrostatic inchworm microsystem with long range translation. Sens Actuators 2004;114(2–3):379–86.
[11] Liu CH, Jywe WY. A four-degree-of-freedom microstage for the compensation of eccentricity of a roundness measurement machine. Int J Mach Tools Manuf 2004;44(4):365–71.
[12] Chu CL, Fan SH. A novel long-travel piezoelectric-driven linear nanopositioning stage. Prec Eng 2006;30(1):85–95.
[13] Jywe WY, Shen JC, Teng YF, Liu CH, Jian YT. Development of a flexure hinge based stack-type five-degree-of-freedom nanometer positioning stage. J Chin Inst Mech Eng 2004;25(6):465–74.
[14] Banning R, de Koning WL, Adriaens HJMTA, Koops RK. State-space analysis and identification for a class of hysteretic systems. Automatica 2001;37(12):1883–92.
[15] Coleman BD, Hodgdon ML. A constitutive relation for rate-independent hysteresis in ferromagnetically soft materials. Int J Eng Sci 1986;24:897–919.
[16] Hodgdon ML. Applications of a theory of ferromagnetic hysteresis. IEEE Transaxtions on Magnetic 1988;24:218–21.